

# CD8 T cell-mediated depletion of HBV surface-antigen-expressing, bilineal-differentiated liver carcinoma cells generates highly aggressive escape variants

Na Qiu<sup>a,b,#</sup>, Akshaya Srikanth<sup>a,#</sup>, Medhanie Mulaw<sup>c</sup>, Umesh Tharehalli<sup>a,d</sup>, Shanthiya Selvachandran<sup>a</sup>, Martin Wagner<sup>a</sup>, Thomas Seufferlein<sup>a</sup>, Katja Stifter<sup>a</sup>, André Lechel<sup>a\*</sup>, and Reinhold Schirmbeck<sup>id a\*</sup>

<sup>a</sup>Department of Internal Medicine I, University Hospital of Ulm, Ulm, Germany; <sup>b</sup>Unit for single-cell Genomics, Medical Faculty, Ulm University, Ulm, Germany; <sup>c</sup>Department of Pediatrics, University Medical Center Groningen, Groningen, The Netherlands; <sup>d</sup>The first Clinical College, Xuzhou Medical University, Xuzhou, Jiangsu, China

## ABSTRACT

The expression of viral antigens in chronic hepatitis B virus (HBV) infection drives continuous liver inflammation, one of the main risk factors to develop liver cancer. HBV developed immune-suppressive functions to escape from the host immune system, but their link to liver tumor development is not well understood. Here, we analyzed if and how HBV surface antigen (HBs) expression in combined hepatocellular-cholangiocarcinoma (cHCC/iCCA) cells influences their antigenicity for CD8 T cells. We randomly isolated liver tumor tissues from  $\text{AlfpCre}^+/\text{Trp53}^{\text{fl/fl}}/\text{Alb-HBs}^+$  tg mice and established primary carcinoma cell lines (pCCL) that showed a bilineal ( $\text{CK7}^+/\text{HNF4}\alpha^+$ ) cHCC/iCCA phenotype. These pCCL uniformly expressed HBs ( $\text{HBs}^{\text{hi}}$ ), and low levels of MHC-I ( $\text{MHC-I}^{\text{lo}}$ ), and were transiently convertible to a high antigenicity ( $\text{MHC-I}^{\text{hi}}$ ) phenotype by IFN- $\gamma$  treatment.  $\text{HBs}^{\text{hi}}/\text{pCCL}$  induced  $\text{HBs}/(\text{K}^b/\text{S}_{190-197})$ -specific CD8 T cells and developed slow-growing tumors in subcutaneously transplanted C57Bl/6J (B6) mice. Interestingly, pCCL-ex cells, established from  $\text{HBs}^{\text{hi}}/\text{pCCL}$ -induced and re-explanted tumors in B6 but not those in immune-deficient  $\text{Rag1}^{-/-}$  mice showed major alterations, like an  $\text{MHC-I}^{\text{hi}}$  phenotype, a prominent growth-biased gene expression signature, a significantly decreased HBs expression ( $\text{HBs}^{\text{lo}}$ ) and a switch to fast-growing tumors in re-transplanted B6 or  $\text{PD-1}^{-/-}$  hosts with an unlocked PD-1/PD-L1 control system. CD8 T cell-mediated elimination of  $\text{HBs}^{\text{hi}}/\text{pCCL}$ , together with the attenuation of the negative restraints of HBs in the tumor cells, like ER-stress, reveals a novel mechanism to unleash highly aggressive  $\text{HBs}^{\text{lo}}/\text{pCCL}$ -ex immune-escape variants. Under certain conditions, HBs-specific CD8 T-cell responses thus potentiate tumor growth, an aspect that should be considered for therapeutic vaccination strategies against chronic HBV infection and liver tumors.

## ARTICLE HISTORY

Received 7 November 2022  
Revised 12 April 2023  
Accepted 14 May 2023

## KEYWORDS

CD8 T cells; ER-stress; HBV surface antigen; immune escape variants; liver carcinoma; tg mice



## Introduction

Risk factors such as chronic infection with hepatitis B virus (HBV) cause persistent liver damage, which can in turn drive the progression of liver cirrhosis, the development of hepatocellular carcinoma (HCC), intrahepatic cholangiocarcinoma (iCCA) or combined cHCC/iCCA.<sup>1,2</sup> In particular, combined cHCC/iCCA is a rare, highly aggressive malignancy that is difficult to diagnose and could arise from different precursors, e.g., through transdifferentiation of hepatocytes, but also from cholangiocytes or putative hepatic stem/progenitor cells.<sup>1</sup>

Little is known about the mechanisms that fail to combat acute HBV infection and trigger the development of chronic infection in some patients.<sup>3</sup> A vaccine, based on recombinant HBV surface antigen particles (HBs), protects recipients from future infections with HBV and reduces the risk of developing HBV-induced liver cancer.<sup>4</sup> However, when HBV infection has


reached a chronic stage, current immune therapies and vaccines are not successful.<sup>3</sup> A major problem is that the virus has developed various strategies to escape from the host immune system, at least in some patients. In particular, HBs display immune-suppressive functions and contribute to the pathogenesis of chronic infection, although HBs are a highly antigenic target for various arms of the immune system.<sup>5-8</sup> Among others, endogenously expressed HBs in hepatocytes cause ER-stress, persistent liver damage and various molecular disorders that critically affect HBV transcription and replication,<sup>9-12</sup> but might also promote tumor progression.<sup>8</sup> Furthermore, most of HBV-specific CD8 T and/or CD4 T cells are severely dysfunctional or exhausted in chronic HBV infection and various HBV mouse models, indicated among others by the upregulation of checkpoint molecules like PD-1 or CTLA-4.

In this study, we established the  $\text{AlfpCre}^+/\text{Trp53}^{\text{fl/fl}}/\text{Alb-HBs}^+$  tg mouse model to determine if and how HBs influence

**CONTACT** Reinhold Schirmbeck  [reinhold.schirmbeck@uni-ulm.de](mailto:reinhold.schirmbeck@uni-ulm.de)  Department of Internal Medicine I, University Hospital of Ulm, Albert Einstein Allee 23; D-89081, Ulm, Germany

<sup>#</sup>N.Q. and A.S. share first authorship

<sup>\*</sup>A.L. and R.S. share senior authorship.

 Supplemental data for this article can be accessed online at <https://doi.org/10.1080/2162402X.2023.2215096>

© 2023 The Author(s). Published with license by Taylor & Francis Group, LLC.

This is an Open Access article distributed under the terms of the Creative Commons Attribution-NonCommercial License (<http://creativecommons.org/licenses/by-nc/4.0/>), which permits unrestricted non-commercial use, distribution, and reproduction in any medium, provided the original work is properly cited. The terms on which this article has been published allow the posting of the Accepted Manuscript in a repository by the author(s) or with their consent.

the antigenicity of liver carcinoma cells for CD8 T cells. The entire coding region of the three HBV surface proteins, i.e., the large (S1-S2-S), the middle (S2-S) and the small surface (S) antigen, was used to generate Alb-HBs<sup>13</sup> and AlfpCre<sup>+</sup>-Trp53<sup>fl/fl</sup>/Alb-HBs<sup>+</sup> tg mice. This leads to a high expression of filamentous lipoprotein particles in hepatocytes, which are inefficiently secreted, accumulate in the ER and cause ER-stress with its associated constraints on the cell phenotype and metabolism.<sup>11,13–15</sup> Alb-HBs tg mice almost exclusively develop HCC.<sup>13</sup> In contrast, intrahepatic deletion of the tumor suppressor gene *Trp53* in AlfpCre<sup>+</sup>-Trp53<sup>fl/fl</sup>/Alb-HBs<sup>+</sup> tg mice leads, in addition to the development of HCC-type tumor areas, also to a pronounced development of iCCA (about 5%) and cHCC/iCCA (about 20%) and, similar to human HBV-related *TP53*-mutant liver carcinoma, to a worsened survival, confirming that the loss of *Trp53* facilitated cHCC/iCCA tumor formation.<sup>16–18</sup> To determine functional tumor/CD8 T-cell interactions, primary HBs-expressing liver carcinoma cell lines (pCCL) were randomly generated *ex vivo* from tumor tissues of AlfpCre<sup>+</sup>-Trp53<sup>fl/fl</sup>/HBs<sup>+</sup> tg mice. We noticed an exclusive outgrowth of cHCC/iCCA-type liver carcinoma cells that were subsequently used to determine the specific changes in the cell surface phenotype (MHC-I expression), the overall gene expression signature, the induction of HBs/(K<sup>b</sup>/S<sub>190–197</sub>)-specific CD8 T-cell responses and the growth properties in subcutaneously transplanted hosts. In pCCL-transplanted B6 mice, we showed a quantitative CD8 T cell-mediated conversion of HBs-expressing HBs<sup>hi</sup>/pCCL to HBs-deficient HBs<sup>lo</sup>/pCCL-ex tumor variants, which were no longer recognized by HBs-specific CD8 T cells. HBs-specific CD8 T cells thus played a crucial role in generating immune-escape variants that lose or down-regulate HBs expression.

## Materials and methods

### Mice

Young (2–3 months) male and female PD-1-deficient (PD1<sup>-/-</sup>), B6.129S7-*Rag1*<sup>tm1Mom</sup>/J (RAG1<sup>-/-</sup>), C57BL/6J, HBs tg mice (C57BL/6J-Tg(Alb1HBV)44Bri/J; JAX stock #002226),<sup>13</sup> AlfpCre<sup>+</sup>-Trp53<sup>fl/fl</sup> tg (AlfpCre × B6.129P2-Trp53tm1Brn/J; JAX stock #008462)<sup>17</sup> and AlfpCre<sup>+</sup>-Trp53<sup>fl/fl</sup>/Alb-HBs<sup>+</sup> tg mice were obtained from our in-house breeding colonies at the Animal Care Facility of Ulm University. Mice were routinely housed in our animal facility under standardized pathogen-free (SPF) conditions. All experiments were performed in accordance with the National Animal Welfare Law and approved by the Committee on the Ethics of Animal Experiments of the University of Ulm and the Regierungspräsidium Tübingen.

### Cell lines

To generate primary liver carcinoma cell lines (pCCL), randomly isolated liver carcinoma developed in different AlfpCre<sup>+</sup>-Trp53<sup>fl/fl</sup>/Alb-HBs<sup>+</sup> tg mice were washed with PBS, cut into small pieces and cultured on collagen-coated plastic plates in DMEM, supplemented with 20% FCS and 1% Penicillin/Streptomycin (#P06–07100; PanBiotech) for 1–2 weeks. Four

pCCL were independently generated from randomly isolated tumor tissues developed in different AlfpCre<sup>+</sup>-Trp53<sup>fl/fl</sup>/Alb-HBs<sup>+</sup> tg mice, which were expanded for 3–5 passages before using them in the experiments. 1 × 10<sup>6</sup> pCCL cells (in 100 µl PBS) were subcutaneously transplanted into hosts, and the outgrowing tumors were re-explanted to generate pCCL-ex. Briefly, the subcutaneous tumors were isolated, cut into small pieces, digested with trypsin, passed through a 40 µm cell strainer and cultured in DMEM supplemented with 10% FCS and 1% Penicillin/Streptomycin. All cell lines were routinely confirmed ‘mycoplasma free’ using a commercial PCR-based mycoplasma test, according the supplier’s instructions (cat no. A3744, AppliChem GmbH, Germany).

### Determination of HBs-specific CD8 T-cell frequencies

Mice were immunized i.m. with 100 µg pCI/S DNA, and K<sup>b</sup>/S<sub>190–197</sub>-specific IFN-γ<sup>+</sup> CD8 T-cell frequencies in the spleen were determined as described previously,<sup>19</sup> using a high-affinity HB-K<sup>b</sup>/S<sub>190–197</sub> variant (A<sub>V</sub>WLSVIWL<sub>M</sub>) and control K<sup>b</sup>/OVA<sub>257–264</sub> (SIINFEKL) peptides (JPT, Berlin, Germany) for stimulation. The frequencies of CD8<sup>+</sup> IFN-γ<sup>+</sup> T cell frequencies were determined by flow cytometry (FCM) using an Attune NxT machine.

### Immunofluorescence

Cells were grown on glass coverslips and fixed with % PFA at 4°C. Unspecific binding of antibodies was blocked with 3% BSA/PBS w/wo 0.3% Triton-X 100 at RT for 1 h. Subsequently, cells were incubated with the primary antibodies (#70-HG15S, Fitzgerald; #181598, Abcam; #sc374229, Santa Cruz) at 4°C overnight, washed and incubated with the corresponding secondary antibodies AP106C (Millipore), A21206 (Thermo Fisher) and A10037 (Sigma) for 1 h and mounted with Prolong Gold antifade reagent (Invitrogen). The cells were imaged with a fluorescence microscope (Keyence BZ X810).

### PCR and qRT-PCR

cDNA was amplified on an ABI 7500 real-time PCR system (Applied Biosystems, Foster City, USA) using iTaq Universal SYBR Green Supermix (Bio-Rad). The primers 5′-GCTCGTGTTACAGGCGGGGTTTTTC-3′ (forward) and 5′-GGTTCCTTGAGCAGGAGTCGTG-3′ (reverse) were used to amplify HBs. Primers 5′-CATCACTGCCACCCAGAAGACTG-3′ (forward) and 5′TGCCAGTGAGCTTCCCGTTCAG-3′ (reverse) were used to amplify GAPDH. The fold change of HBs-specific expression was determined by the ΔΔCT method.

PCR was performed in a C1000 Touch Thermal Cycler, and the products were run on 1.5% agarose gels.

### Gene expression analysis

Total RNA was isolated from the indicated tumor cell lines with RNeasy® Mini Kit (Qiagen, Germany) according to the manufacturer’s protocol. The sample quality was analyzed

using a bioanalyzer (Agilent Technologies, Santa Clara, USA) with the RNA6000 Nano kit (Agilent Technologies, Santa Clara, CA, USA) according to the manufacturer's guidelines. Samples with an RIN (RNA integrity number) higher than 7.0 were used for further analysis. Gene expression analysis was carried out using the SurePrint G3 Mouse Gene Expression 8 × 60 K Microarray (Design ID 028005; Agilent Technologies, Santa Clara, CA, USA). Samples were labeled with the Low Input Quick Amp Labeling Kit (Agilent Technologies) according to the manufacturer's guidelines. Slides were scanned in a G2565CA microarray scanner and extracted with the Feature Extraction Software (v.10.7.3.1, Agilent Technologies).

### Bioinformatic analyses

Raw microarray data were background corrected and quantile normalized using the R and Bioconductor package limma (<https://www.R-project.org>). Gene Set Enrichment Analysis (GSEA) was performed using a standalone Java implementation of the package.<sup>20</sup> Differences in gene expression were considered to be significant at a Benjamini–Hochberg (BH) adjusted *p*-value smaller than 0.05. Pathway network analysis was performed within GSEA, and the plot was generated using Cytoscape.<sup>21</sup> Genesets were considered significantly enriched at an FDR *q*-value of <25%. Heatmaps were generated using Heatplus (Ploner a. 2021. Heatplus: Heatmaps with row and/or column covariates and colored clusters; R package version 3.2.0; <https://github.com/alexploner/Heatplus>).

### Statistical analysis

Data analysis was performed with the GraphPad Prism version 8. For calculating statistical significance, differences were examined by unpaired *t*-test, one-way ANOVA with Tukey's multiple comparisons test. Data are presented as the mean ± standard error. A value of *p* < 0.05 (\*), *p* < 0.01 (\*\*), *p* < 0.001 (\*\*\*) and *p* < 0.0001 (\*\*\*\*) was considered statistically significant.

## Results

### Characterization of liver carcinoma cells

AlfpCre<sup>+</sup>-Trp53<sup>fl/fl</sup> mice were crossed with Alb-HBs tg mice to generate the AlfpCre<sup>+</sup>-Trp53<sup>fl/fl</sup>/Alb-HBs<sup>+</sup> tg mouse model that represents continuous liver damage through overexpression of HBs in the liver, particularly in the *Endoplasmic Reticulum* (ER) of transgenic cells, indicated by elevated serum alanine transaminase (ALT) levels in the blood.<sup>11,13</sup> As compared to Alb-HBs tg mice, the depletion of *Trp53*<sup>-/-</sup> in AlfpCre<sup>+</sup>-Trp53<sup>fl/fl</sup>/Alb-HBs<sup>+</sup> tg mice resulted in an accelerated development of liver tumors (Figure 1a) composed of HCC (76.5%), but also of iCCA (4.9%) and cHCC/iCCA (18.6%) (Figure 1b).

Liver tumor tissue was isolated from different AlfpCre<sup>+</sup>-Trp53<sup>fl/fl</sup>/Alb-HBs<sup>+</sup> tg mice, and primary carcinoma cell lines (pCCL) were established *in vitro* as described in M&M. These pCCL (e.g., pCCL-1) showed a bilineal differentiation, indicated by the co-expression of the hepatocyte marker HNF4α and the cholangiocyte marker CK7 (Figure 1c). Furthermore, pCCL showed a low antigenicity

surface phenotype with low levels of MHC-I (H2-K<sup>b</sup>) and basal levels of co-inhibitory PD-L1 (Figure 1d). This MHC-I<sup>lo</sup> phenotype was maintained during prolonged cell culture *in vitro* (Fig. S1A). The dysregulated MHC-I<sup>lo</sup> expression in the pCCL was not defined by genetic alterations and could be transiently reconstituted for 4–6 d by treating them for 20 h with 20 ng/ml recombinant IFN-γ (pCCL-IFNγ; Figure 1e).<sup>19</sup>

### Generation of MHC-I<sup>hi</sup> HBs<sup>lo</sup>/pCCL-ex variants.

Subcutaneously transplanted pCCL was efficiently grafted as solid tumors in B6 mice, though the growth rate was low and tumor sizes of 10 mm were not reached even after 40–60 d post transplantation (Figure 2a). When carcinoma cells were re-isolated from these tumors, the corresponding pCCL-ex showed an altered MHC-I<sup>hi</sup> phenotype, while PD-L1 expression remained at basal levels (Figure 2b). In contrast to the transient, IFNγ-induced MHC-I<sup>hi</sup> phenotype in pCCL-IFNγ (Figure 1e), the upregulation of MHC-I expression was stable during prolonged cell culture of pCCL-ex (Figure 2b; Fig. S1B). As compared with B6 mice, equal numbers of pCCL-1 grew much faster in transplanted Rag1<sup>-/-</sup> mice, which lack mature B and T lymphocytes, and cell lines derived from re-isolated tumor explants, like the pCCL-1-ex-Rag, still expressed the MHC-I<sup>lo</sup> phenotype (Figure 2 a-d). In conclusion, the adaptive immune system in B6 mice might play a prominent role in generating MHC-I<sup>hi</sup> tumor cells.

### pCCL-ex show an enhanced aggressiveness in re-transplanted hosts.

We next investigated whether the MHC-I<sup>hi</sup> phenotype in pCCL-ex and/or in pCCL-IFNγ has an impact on their outgrowth in transplanted B6 mice. Equal numbers of subcutaneously transplanted pCCL-1-IFNγ or pCCL developed into solid tumors with a similar kinetics, but pCCL-1-ex grew much faster than pCCL-1 or pCCL-1-IFNγ and reached a tumor diameter of 10 mm between day 20–30 post transplantation in B6 mice (Figure 2e). This strongly indicated that pCCL-1 and pCCL-1-IFNγ, but not pCCL-1-ex interact with the immune system to retard tumor growth *in vivo*.

Next, we transplanted equal numbers of pCCL-1, pCCL-1-IFNγ and pCCL-1-ex into PD-1<sup>-/-</sup> mice, as we expected that the destruction of the PD-1/PD-L1 co-inhibitory pathway could enhance effector CD8 T-cell functions and thereby facilitate the elimination of transplanted tumor cells.<sup>19</sup> Indeed, pCCL-1-IFNγ were efficiently rejected in transplanted PD-1<sup>-/-</sup> mice, and also the growth of parental pCCL-1 was impeded in the absence of PD-1/PD-L1 co-inhibition (Figure 2f). In clear contrast, pCCL-1-ex developed tumors in PD-1<sup>-/-</sup> and B6 mice with a similar kinetics (Figure 2e,f), suggesting that the immune system interacts with pCCL-1 and pCCL-1-IFNγ, but not with pCCL-1-ex tumors.

### Analysis of intrinsic gene expression signatures in pCCL-ex

Gene expression analysis was performed to identify differentially expressed genesets that could explain the increased aggressiveness of pCCL-ex. Unsupervised hierarchical clustering-based heatmaps of significantly differentially expressed

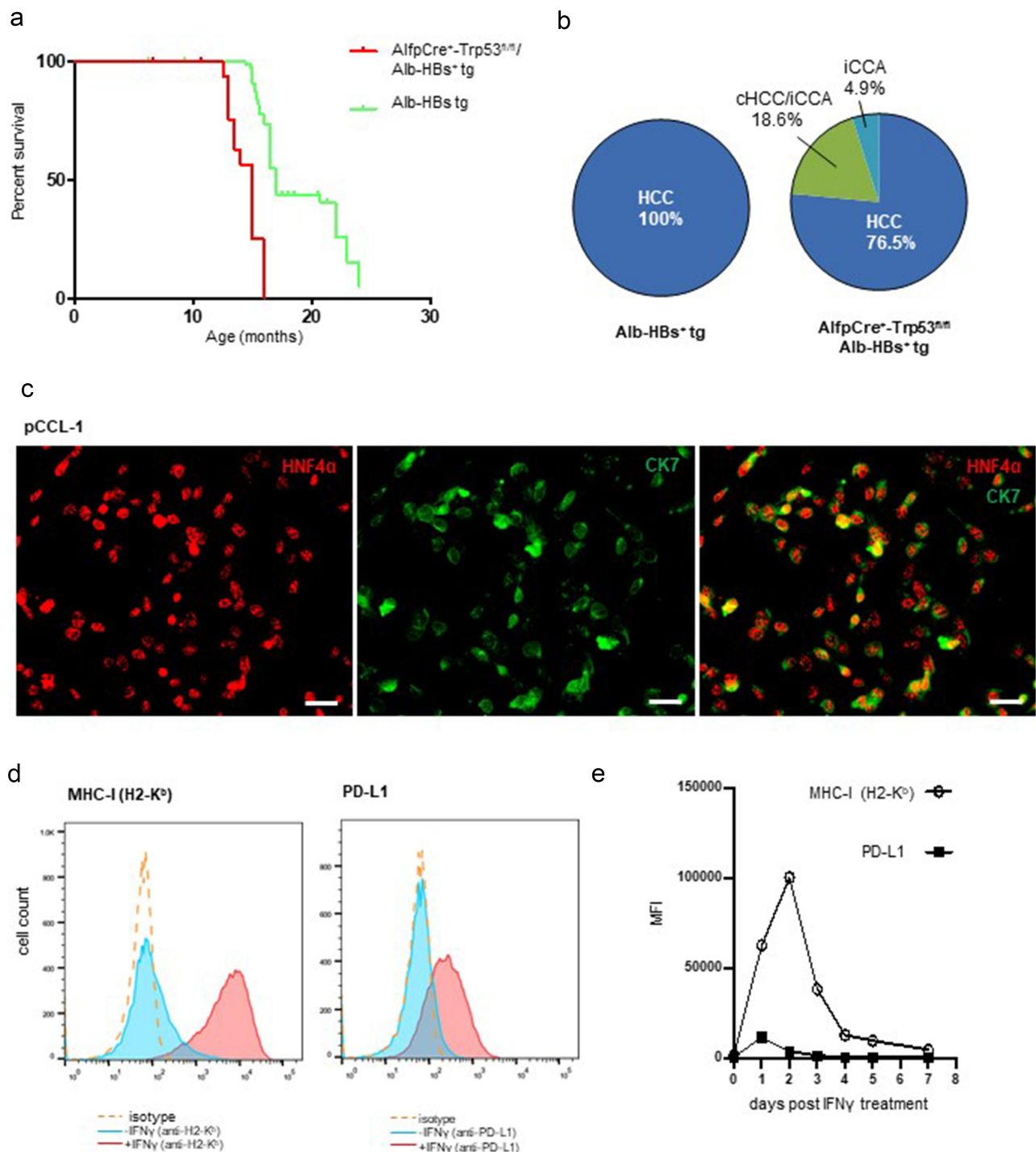


**Figure 1.** Characterization of liver carcinoma cell lines. (a) Tumor-free survival curve of Alb-HBs<sup>+</sup> (n = 79) and AlfpCre<sup>+</sup>-Trp53<sup>fl/fl</sup>/Alb-HBs<sup>+</sup> tg mice (n = 22). (b) Pie charts representing the specific distribution of liver carcinoma differentiation in Alb-HBs<sup>+</sup> and AlfpCre<sup>+</sup>-Trp53<sup>fl/fl</sup>/Alb-HBs<sup>+</sup> tg mice. (c) Primary liver carcinoma cells (pCCL) were established from liver tumors developed in AlfpCre<sup>+</sup>-Trp53<sup>fl/fl</sup>/Alb-HBs<sup>+</sup> tg mice and analyzed for coexpression of HNF4 $\alpha$  and CK7 by immunofluorescence as described in M&M. One representative photograph of each staining is shown. Scale bar: 20  $\mu$ m. (d) A representative pCCL-1 was treated with 20 ng/mL recombinant mouse IFN $\gamma$  for 20 h or remained untreated, followed by FCM of MHC-I (H2-K<sup>b</sup>) and PD-L1 expression. One representative histogram out of three independent experiments is shown. (e) Similarly, pCCL-1 were treated with 20 ng/mL IFN $\gamma$  for 20 h, washed with PBS and cultured for up to 7 d. The surface expression of MHC-I (open circles) and PD-L1 (closed squares) was measured by FCM at the indicated time points. One representative histogram out of three independent experiments is shown. MFI, Mean Fluorescent Intensity.

genes showed that pCCL and pCCL-IFN $\gamma$  were more similar as compared to pCCL-ex (Figure 3a; Table S1A,B). As expected, the comparison between pCCL versus pCCL-IFN $\gamma$  showed 283 significant differentially expressed genes, of which 281 genes were upregulated, and only 2 genes were downregulated in

pCCL-IFN $\gamma$  (Figure 3b; Table S1A,B).<sup>19</sup> In clear contrast, pCCL versus pCCL-ex showed a higher number of significant differentially expressed genes, i.e., 1163 genes, of which 710 genes were upregulated, and 453 genes were downregulated in pCCL-ex (Figure 3b; Table S1A,B). Sixty-one genes were found

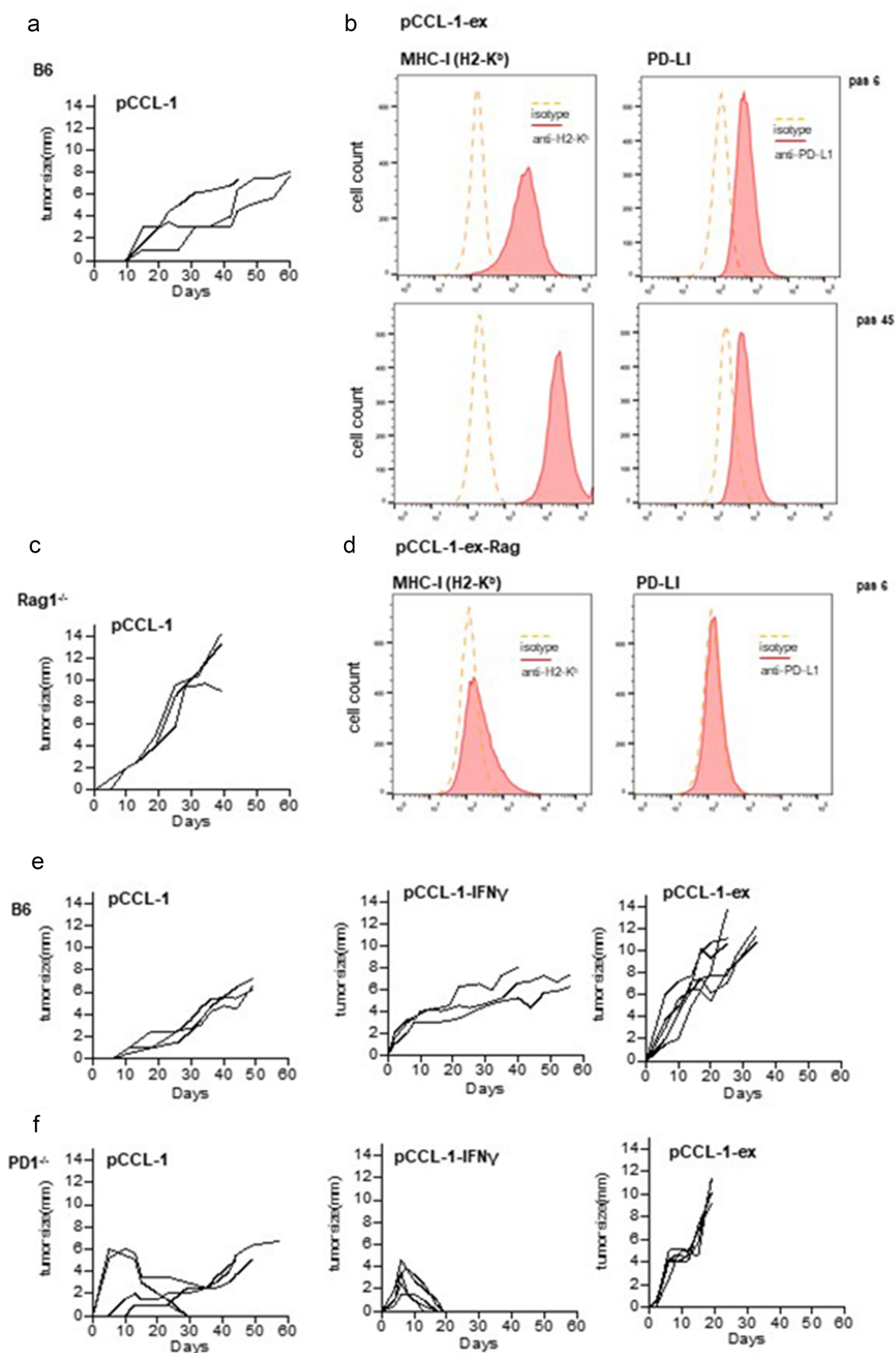


**Figure 2.** Growth of pCCL in transplanted B6 mice. (a–d) Equal numbers ( $1 \times 10^6$ ) pCCL-1 were subcutaneously transplanted into the left flank of B6 (a) or Rag1<sup>-/-</sup> mice (c) ( $n = 3$ ), and tumor growth was monitored. (b,d) Tumors were explanted from these transplanted mice and cultured *in vitro*, generating pCCL-ex and pCCL-ex-Rag, respectively. The cell surface expression of H2-K<sup>b</sup> and PD-L1 was assessed at passages 6 and 45, respectively (c,d). A representative histogram (out of three independently generated pCCL-ex and pCCL-ex-Rag) is shown. (e,f) Equal numbers ( $1 \times 10^6$ ) of pCCL, pCCL-IFN $\gamma$  (pCCL pretreated for 20 h with 20 ng/mL IFN $\gamma$ ) and pCCL-ex were subcutaneously transplanted into B6 ( $n = 3-6$ ) (e) and PD1<sup>-/-</sup> mice ( $n = 5$ ) (f) and tumor growth was monitored.

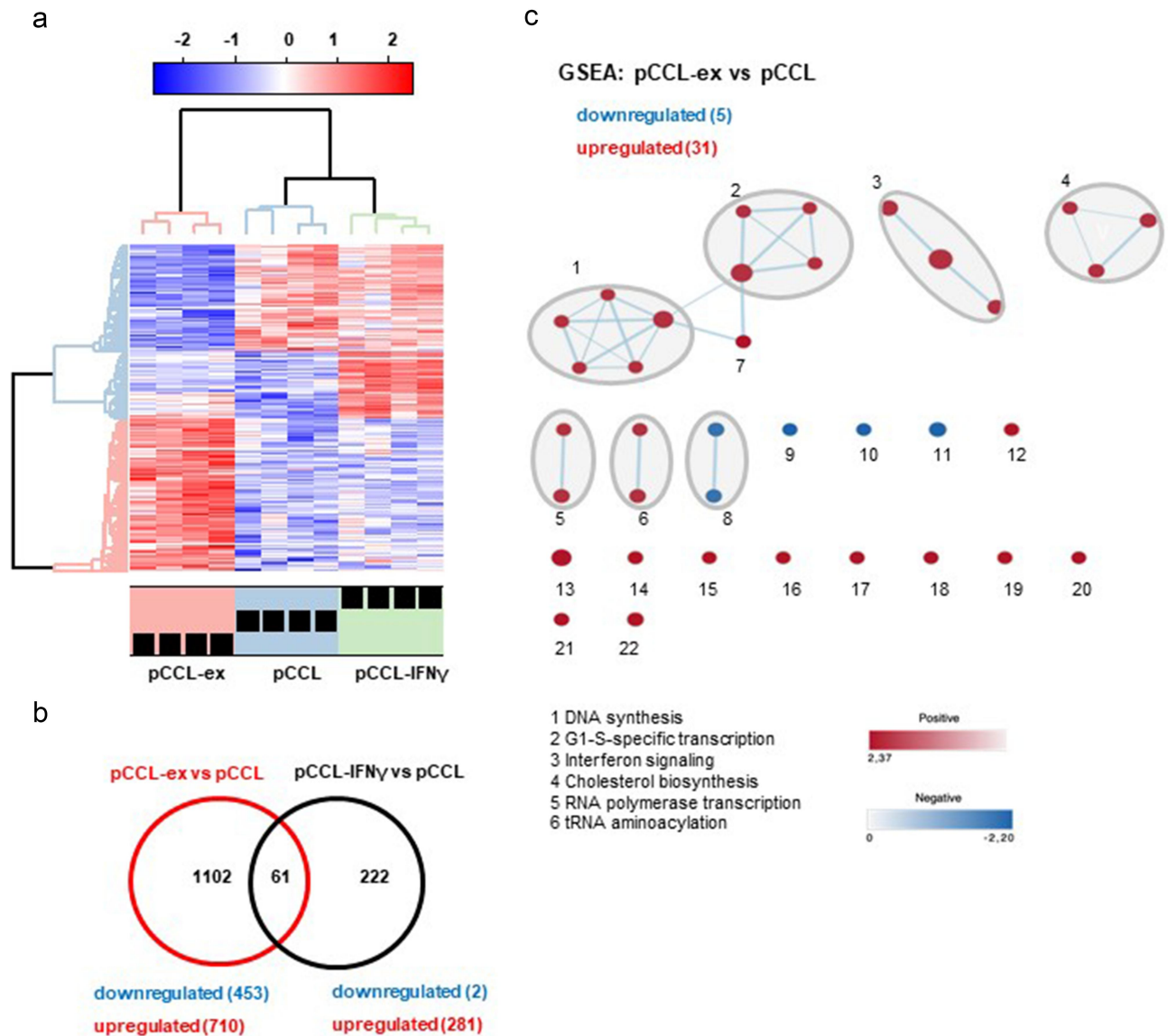


**Figure 3.** Gene expression signatures of different tumor cell lines. (a) The gene expression pattern was determined in four independently generated pCCL, IFN $\gamma$  pretreated pCCL-IFN $\gamma$  and pCCL-ex, respectively. Unsupervised hierarchical clustering based on significant differentially expressed genes in pCCL, pCCL-IFN $\gamma$  and pCCL-ex is shown. The red label indicates upregulated genes, while the blue label indicates downregulated genes. (b) The Venn diagram shows the number of significant differentially expressed genes in the pCCL-ex versus pCCL and pCCL-IFN $\gamma$  versus pCCL comparisons. Furthermore, the numbers of up- and down-regulated genes are indicated. (c) GSEA and reactome pathway network analysis were performed on the 1163 significantly differentially expressed genes, determined in the comparison of pCCL-ex versus pCCL. The significantly enriched and differentially regulated pathway-associated genesets are described in detail in Table S1D,F.

to be significantly upregulated in common between pCCL-IFN $\gamma$  and pCCL-ex and contained among other genes involved in antigen presentation like TAP1 (Figure 3b; Table S1C).

We next performed geneset enrichment (GSEA) and pathway network analyses between significantly enriched genesets in pCCL versus pCCL-ex (Figure 3c). This allowed us to assess whether the relative ranking of genes provides evidence of a nonrandom aggregation and skewness toward the top list of either the upregulated or downregulated ranks of genes and thus highlights their enrichment in biological networks.<sup>21</sup> As compared with pCCL, 31 genesets were upregulated and 5 genesets downregulated in pCCL-ex (Table S1D) and showed a prominent enrichment of genesets in networks associated with an enhanced tumor

growth profile, like DNA synthesis or G1-S-specific transcription (Figure 3c, Table S1F). Confirmatory, equal numbers of pCCL-1-ex showed a faster tumor growth *in vivo* in transplanted Rag1<sup>-/-</sup> mice than pCCL-1 (Fig. S2). The pCCL-ex also showed an enhanced expression of genesets associated with interferon signaling and antigen presentation that matched with the increased cell surface expression of MHC-I molecules (Figure 3c, Table S1F) but did not reach the highly focused enrichment of the interferon signaling network in pCCL-IFN $\gamma$  versus pCCL (Fig. S3; Table S1E,G).<sup>19</sup> Overall, these analyses could explain, at least in part, why pCCL-ex developed fast growing tumors upon re-transplantation in B6 mice, but did not explain why the immune system failed to control the growth of this MHC-I<sup>hi</sup> phenotype pCCL-ex.

### The pCCL-ex variants lose overexpression of HBs

Endogenously expressed HB are a strong cellular antigen in immune-competent B6 mice. Both, pCCL and pCCL-IFN $\gamma$  efficiently expressed HBs transcripts, while pCCL-ex showed a significantly decreased expression (Figure 4 A,Ba,b). Furthermore, immunofluorescence analyses confirmed that the HBs protein was strongly reduced in pCCL-ex as compared to parental pCCL (Figure 4 Cc), while the co-expression of CK7 and HNF4 $\alpha$  was maintained (Fig. S4). As compared to parental pCCL, HBs expression was preserved in pCCL-ex-Rag that were established from pCCL-induced tumors in immune-deficient Rag1<sup>-/-</sup> mice (Fig. S5; Figure 4Cc). This further indicated that HBs-specific immune responses were involved in the generation of HBs<sup>lo</sup>/pCCL-ex. Confirmatory, B6 mice transplanted with equal numbers of pCCL or pCCL-IFN $\gamma$ , but not with pCCL-ex elicited a HBs/(K<sup>b</sup>/S<sub>190-197</sub>)-specific CD8 T-cell response (Figure 4Dd). The level of HBs-expression in pCCL and pCCL-IFN $\gamma$  but not in pCCL-ex was thus sufficient to cross-prime HBs/(K<sup>b</sup>/S<sub>190-197</sub>)-specific CD8 T cells by cell-based immunization. Furthermore, HBs/(K<sup>b</sup>/S<sub>190-197</sub>)-specific CD8 T cells primed in B6 mice by pCI/S DNA vaccination (Figure 4Ee) rejected subcutaneously transplanted HBs<sup>hi</sup>/pCCL-1 but not HBs<sup>lo</sup>/pCCL-1-ex (Figure 4Ff). The prominent decrease of HBs-expression in HBs<sup>lo</sup>/pCCL-1-ex thus prevented priming of HBs-specific CD8 T cells as well as their recognition by HBs-specific CD8 T cells.

### Discussion

Many tumors develop mechanisms to escape from recognition and elimination by CD8 T cells<sup>22</sup>. This is highly relevant for virus-induced tumors, in which viral antigens are foreign and efficiently recognized by the cellular immune system. Here, we describe a CD8 T cell-mediated escape mechanism for HBs-expressing bilineal differentiated cHCC/iCCA liver carcinoma cells (HBs<sup>hi</sup>/pCCL), established from spontaneously developing liver tumors in AlfpCre<sup>+</sup>-Trp53<sup>fl/fl</sup>/Alb-HBs<sup>+</sup> tg mice (Fig. S6). Upon transplantation into B6 mice, HBs-expressing HBs<sup>hi</sup>/pCCL grew into solid subcutaneous tumors and primed HBs/(K<sup>b</sup>/S<sub>190-197</sub>)-specific CD8 T cells. Concomitantly, these CD8 T cells interacted with the transplanted HBs<sup>hi</sup>/pCCL that finally resulted in the quantitative accumulation of HBs<sup>lo</sup>/pCCL-ex in the tumors, a scenario not seen in pCCL-transplanted Rag1<sup>-/-</sup> mice lacking T- and B-cells (Fig. S6). The HBs<sup>lo</sup>/pCCL-ex were no longer accessible to HBs-specific CD8 T cells and unleashed an aggressive phenotype in secondary transplanted hosts, though they expressed a co-induced MHC-I<sup>hi</sup> phenotype (Fig. S6). However, the origin of HBs<sup>lo</sup>/pCCL-ex is unknown. We showed that strong interferon signals, which often down-regulate promoter activities,<sup>23</sup> did not affect the albumin promoter-driven expression of HBs in HBs<sup>hi</sup>/pCCL-IFN $\gamma$ . HBs<sup>lo</sup>/pCCL-ex thus arise in response to HBs-specific CD8 T cells in HBs<sup>hi</sup>/pCCL-transplanted B6 mice, e.g., by events that might change the overall DNA methylation status.<sup>24</sup> The significantly decreased expression of HBs in HBs<sup>lo</sup>/pCCL-ex apparently rescued them from the HBs-induced continuous ER-stress and correlated with a change in the specific gene

expression signature toward enhanced tumor growth. In particular, geneset networks involved in DNA synthesis and G1-S transcription were upregulated in HBs<sup>lo</sup>/pCCL-ex, as compared with parental HBs<sup>hi</sup>/pCCL, and correlated with an enhanced tumor growth in immune-deficient Rag1<sup>-/-</sup> mice. Noticeable, pre-existing HBs-specific CD8 T cells in pCI/S-immunized mice quantitatively eliminated transplanted HBs<sup>hi</sup>/pCCL. This suggested that transplantation of pCCL into B6 mice induced a functionally and/or temporally balanced HBs-specific CD8 T-cell response, likely with the interplay of immune suppressive cell types, which regulate the selective outgrowth of HBs<sup>lo</sup>/pCCL-ex in developing tumors. Concordantly, HBs<sup>lo</sup>/pCCL-ex unleashed their high aggressiveness in secondary transplanted hosts, but not in the initial pCCL-transplanted B6 hosts.

The CD8 T cell-mediated generation of HBs-deficient tumor-escape variants, like the HBs<sup>lo</sup>/pCCL-ex in this study, could impact novel immunotherapies against HBV-induced liver carcinoma. For example, particularly HBs was used as tumor-specific antigen to target HBV-induced HCC by novel T-cell therapies.<sup>25,26</sup> Redirected T cells expressing engineered high-affinity T-cell receptors, e.g., specific for the viral HBs, showed a promising efficacy in patients with primary HBV-induced HCC or HBV-induced HCC recurrence after liver transplantations.<sup>25,26</sup> Immune-mediated loss of HBs expression in a subset of liver tumor cells would thus complicate this strategy.

HBs<sup>hi</sup>-induced ER-stress in hepatocytes could contribute to various immune-suppressive events or molecular disorders that keep up persistent HBV infection and the progression to liver tumors.<sup>8-12</sup> The high amount of HBs produced in infected hepatocytes and released into circulation is most impressive for chronic HBV infection. HBs consist primarily of noninfectious lipoprotein particles and filaments, which could reach quantities of up to >300  $\mu$ g/ml.<sup>27</sup> HBs particles efficiently target and pass cell membranes and directly interfere with cell surface-associated as well as endogenous signaling pathways.<sup>5,7,28</sup> For example, HBs particles were efficiently taken up and processed for MHC-I-restricted presentation in various cell types.<sup>29</sup> This could lead to an (over)presentation of HBs-specific MHC-I epitopes on different nonprofessional antigen-presenting cells (APCs) including the tolerogenic milieu of the liver that 'over-stimulate' or exhaust potential *de novo* primed HBs-specific CD8 T cells. Furthermore, the clearance of HBs from chronically infected patients is usually associated with the appearance of anti-HBs antibodies (seroconversion) and increased HBV-specific T-cell responses.<sup>30</sup> This exemplified that overexpression of HBs negatively affects the immune system. However, clearance of circulating HBs in a HBV replication-competent transgenic mouse model, either via spontaneous seroconversion or therapeutic monoclonal antibodies, had only a minimal effect on the expansion and functionality of naive, HBV-specific CD8 T cells undergoing intrahepatic priming.<sup>31</sup> This indicates that HBs is not the sole regulator of anti-viral immune responses in humans, as chronic HBV infection causes many dysfunctions in the adaptive and innate immune system, involving very different cell types like myeloid-derived suppressor cells, regulatory CD4 Treg cells or T cells.

Despite the difficult diagnosis and low incidence rates, HBs-expression was detectable in 17–58% of cHCC/iCCA

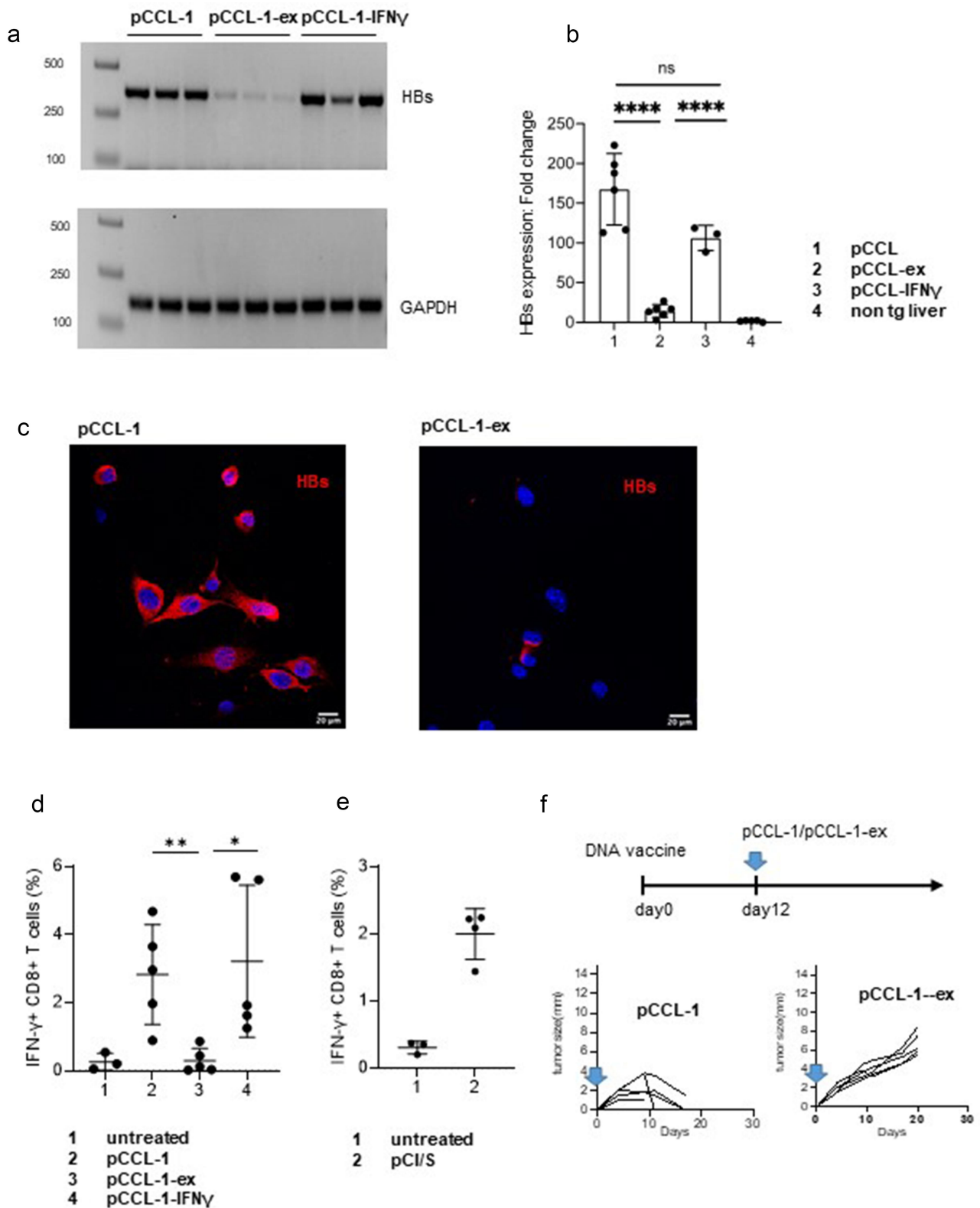


**Figure 4.** Characterization of the HBs-specific antigenicity. The mRNA levels of HBs were measured in representative pCCL-1, pCCL-1-ex and pCCL-1-IFN $\gamma$  in triplicates by conventional PCR and agarose gel electrophoresis (a) or by RT-qPCR (b) ( $n = 3-6$ /group). (c) Representative pCCL-1 and pCCL-1-ex were analyzed for HBs expression (red) by immunofluorescence staining. Scale bar: 20  $\mu$ m. Furthermore, nuclei were stained with DAPI (blue). (d) B6 mice were injected with equal numbers ( $1 \times 10^6$ ) of pCCL-1, pCCL-1-ex or pCCL-1-IFN $\gamma$  ( $n = 5$ ) or remained untreated ( $n = 3$ ). After 12 days,  $K^b/S_{190-197}$ -specific IFN- $\gamma^+$  CD8 $^+$  T-cell frequencies ( $\pm$ SD) in the spleen (%) are shown. The non-specific  $K^b/OVA_{257-264}$  frequencies, usually  $\leq 0.2\%$ , were subtracted from the presented values. (e) B6 mice were immunized with pCI/S ( $n = 4$ ) or remained untreated ( $n = 3$ ), and  $K^b/S_{190-197}$ -specific IFN- $\gamma^+$  CD8 $^+$  T cells were determined as described above. (f) B6 mice ( $n = 5$ ) were immunized with pCI/S and, after 12 days, subcutaneously transplanted with equal numbers ( $1 \times 10^6$ ) of pCCL-1 or pCCL-1-ex. Tumor growth was monitored. ns, not significant; \* $p < 0.05$ ; \*\* $p < 0.01$ ; \*\*\*\* $p < 0.0001$ .



tumors,<sup>32,33</sup> confirming a prominent proportion of HBV-induced cHCC/iCCA carcinoma. The continuous presence of secreted HBs or HBs-induced ER-stress could thus promote malignant progression of HBV-induced liver carcinoma.<sup>5,8,34</sup> Defective HBs antigens with mutations, e.g., in the immunodominant HBs<sub>124–147</sub> ‘a’ determinant or in the preS domain, are not or inefficiently targeted by anti-HBs serum antibodies and/or trigger a disturbed assembly and secretion of empty HBs particles and virions in the ER.<sup>5</sup> In particular, mutations in the preS domain were associated with an increased risk of HCC.<sup>34</sup> In contrast, spontaneous loss of HBs has been reported in patients with chronic HBV infection and assigned to functional anti-HBV immune responses, HBV cure and a trend toward a lower incidence in the development of liver tumors.<sup>30,35–37</sup> For example, in a population-based cohort study with 1271 Alaska Native patients chronically infected with HBV and followed for an average of 19.6 y, it was shown that about 158 (12%) lost HBs.<sup>36</sup> The incidence of HCC development after clearance of HBs over time was significantly lower than in the remaining HBs-positive patients. However, HBV DNA was still detectable in the sera of 28 (18%) of those who cleared HBs in a median of 3.6 y after clearance.<sup>36</sup> It is unknown if the loss of HBs in chronically HBV-infected liver tissues induces intrinsic alterations in the cells *per se* and/or affects their communication with the immune system that, at least partially, prevents HCC development. The cellular mechanisms induced by the loss of HBs thus might differ in HBV<sup>+</sup> liver cells prone to developing liver tumors and in established cHCC/iCCA tumor cells.

## Conclusion

In summary, our data identified an immune-escape mechanism triggered primarily by the CD8 T cell-mediated eradication of HBs<sup>hi</sup> tumor cells and the concomitant accumulation of highly aggressive HBs<sup>lo</sup> cHCC/iCCA-type tumor cells. These findings could be helpful for the design of therapeutic vaccination strategies against chronic HBV infection and liver tumors, as we demonstrated that HBs-specific CD8 T-cell responses could potentiate tumor growth/escape.

## Acknowledgments

We thank Dr T. Honjo (Department of Immunology and Genomic Medicine, Kyoto University, Kyoto, Japan) for PD-1<sup>-/-</sup> mice and Dr F. Chisari (Professor Emeritus Department of Immunology and Microbiology, The Scripps Research Institute, La Jolla, USA) for HBs tg mice.

## Disclosure statement

No potential conflict of interest was reported by the authors.

## Funding

This work was supported by a grant from the Deutsche Forschungsgemeinschaft: Graduiertenkolleg (GRK) 2254 ‘Heterogeneity and Evolution in Solid Tumors (HEIST)’ to A.L. and R.S. and a grant from the Boehringer Ingelheim Ulm University Biocenter (BIU) to M.W., K.S. and

TS. N.Q. is an MD candidate at Ulm University. Her work is submitted in partial fulfillment of the requirement for her MD thesis.

## ORCID

Reinhold Schirmbeck  <http://orcid.org/0000-0001-6853-8091>

## Authorship contributions

N.Q., U.T., A.S., S.S., K.S. and A.L. performed experiments, researched and interpreted data

N.Q. and M.M. performed biocomputational analyses

M.W., T.S., K.S., A.L. and R.S. conceived the experiments, secured funding, discussed and interpreted data

N.Q., K.S., A.L. and R.S. wrote manuscript

All authors edited and approved the manuscript.

## Data availability statement

All data relevant to this study are included in the article or uploaded as supplemental files. The original raw microarray datasets are accessible via GEO accession GSE215059; <https://www.ncbi.nlm.nih.gov/geo/query/acc.cgi?acc=GSE215059>

## References

1. Stavra C, Rush H, Ross P. Combined hepatocellular cholangiocarcinoma (CHCC-CC): an update of genetics, molecular biology, and therapeutic interventions. *J Hepatocell Carcinoma*. 2018;6:11–21. doi:10.2147/JHC.S159805.
2. Llovet JM, Kelley RK, Villanueva A, Singal AG, Pikarsky E, Roayaie S, Lencioni R, Koike K, Zucman-Rossi FR. Hepatocellular carcinoma. *Nat Rev Dis Primers*. 2021;7(1):6. doi:10.1038/s41572-020-00240-3.
3. Lee HW, Chan H-Y. Unresolved issues of immune tolerance in chronic hepatitis B. *J Gastroenterol*. 2020;55(4):383–389. doi:10.1007/s00535-020-01665-z.
4. Flores JE, Thompson AJ, Ryan M, Howell J. The global impact of hepatitis b vaccination on hepatocellular carcinoma. *Vaccines (Basel)*. 2022;10(5):793. doi:10.3390/vaccines10050793.
5. Wu CC, Chen YS, Cao L, Chen XW, Lu MJ. Hepatitis B virus infection: defective surface antigen expression and pathogenesis. *World J Gastroenterol*. 2018;24(31):3488–3499. doi:10.3748/wjg.v24.i31.3488.
6. Li YW, Yang FC, Lu HQ, Zhang JS. Hepatocellular carcinoma and hepatitis B surface protein. *World J Gastroenterol*. 2016;22(6):1943–1952. doi:10.3748/wjg.v22.i6.1943.
7. Zhu D, Liu L, Yang D, Fu S, Bian Y, Sun Z, He J, Su L, Zhang L, Peng H, et al. Clearing persistent extracellular antigen of hepatitis B virus: an immunomodulatory strategy to reverse tolerance for an effective therapeutic vaccination. *J Immunol*. 2016;196(7):3079–3087. doi:10.4049/jimmunol.1502061.
8. Wu S, Ye S, Lin X, Chen Y, Zhang Y, Jing Z, Liu W, Chen W, Lin X, Lin X. Small hepatitis B virus surface antigen promotes malignant progression of hepatocellular carcinoma via endoplasmic reticulum stress-induced FGF19/JAK2/STAT3 signaling. *Cancer Lett*. 2021;499:175–187. doi:10.1016/j.canlet.2020.11.032.
9. Chen H, Mu M, Liu Q, Hu H, Tian C, Zhang G, Li Y, Yang F, Lin S. Hepatocyte endoplasmic reticulum stress inhibits hepatitis B virus secretion and delays intracellular hepatitis B virus clearance after entecavir treatment. *Front Med*. 2021;7:589040. doi:10.3389/fmed.2020.589040.
10. Kim SY, Kyaw YY, Cheong J. Functional interaction of endoplasmic reticulum stress and hepatitis B virus in the pathogenesis of liver diseases. *World J Gastroenterol*. 2017;23(43):7657–7665. doi:10.3748/wjg.v23.i43.7657.

11. Chisari FV, Filippi P, Buras J, McLachlan A, Popper H, Pinkert CA, Palmiter RD, Brinster RL. Structural and pathological effects of synthesis of hepatitis B virus large envelope polypeptide in transgenic mice. *Proc Natl Acad Sci U S A*. 1987;84(19):6909–6913. doi:10.1073/pnas.84.19.6909.
12. Deng F, Xu G, Cheng Z, Huang Y, Ma C, Luo C, Yu C, Wang J, Xu X, Liu S, et al. Hepatitis B surface antigen suppresses the activation of nuclear factor kappa B pathway via interaction with the TAK1-TAB2 complex. *Front Immunol*. 2021;12:618196. doi:10.3389/fimmu.2021.618196.
13. Chisari FV, Klopchin K, Moriyama T, Pasquinelli C, Dunsford HA, Sell S, Brinster RL, Palmiter RL, Palmiter RD. Molecular pathogenesis of hepatocellular carcinoma in hepatitis B virus transgenic mice. *Cell*. 1989;59(6):1145–1156. doi:10.1016/0092-8674(89)90770-8.
14. Choi YM, Lee SY, Kim BJ. Naturally occurring hepatitis B virus mutations leading to endoplasmic reticulum stress and their contribution to the progression of hepatocellular carcinoma. *Int J Mol Sci*. 2019;20(3):597. doi:10.3390/ijms20030597.
15. Li Y, Xia Y, Cheng X, Kleiner DE, Hewitt SM, Sproch J, Li T, Zhuang H, Liang TJ. Hepatitis B surface antigen activates unfolded protein response in forming ground glass hepatocytes of chronic hepatitis B. *Viruses*. 2019;11(4):386. doi:10.3390/v11040386.
16. Amaddeo G, Cao Q, Ladeiro Y, Imbeaud S, Nault JC, Jaoui D, Mathe YG, Laurent C, Laurent A, Bioulac-Sage P, et al. Integration of tumour and viral genomic characterizations in HBV-related hepatocellular carcinomas. *Gut*. 2015;64(5):820–829. doi:10.1136/gutjnl-2013-306228.
17. Katz SF, Lechel A, Obenauf AC, Begus-Nahrman Y, Kraus JM, Hoffmann EM, Duda J, Eshraghi P, Hartmann D, Liss B, et al. Disruption of Trp53 in livers of mice induces formation of carcinomas with bilineal differentiation. *Gastroenterology*. 2012;142(5):1229–39.e3. doi:10.1053/j.gastro.2012.02.009.
18. Liu Y, Xin B, Yamamoto M, Goto M, Ooshio T, Kamikokura Y, Tanaka Hm Meng L, Mizukami Y, Okada Y, Mizukami Y, et al. Generation of combined hepatocellular-cholangiocarcinoma through transdifferentiation and dedifferentiation in p53-knockout mice. *Cancer Sci*. 2021;112(8):3111–3124. doi:10.1111/cas.14996.
19. Stifter K, Krieger J, Ruths L, Gout J, Mulaw M, Lechel A, Kleger A, Seufferlein T, Wagner M, Schirmbeck R. IFN- $\gamma$  treatment protocol for MHC-I(Io)/PD-L1(+) pancreatic tumor cells selectively restores their TAP-mediated presentation competence and CD8 T-cell priming potential. *J Immunother Cancer*. 2020;8(2):e000692. doi:10.1136/jitc-2020-000692.
20. Subramanian A, Tamayo P, Mootha VK, Mukherjee S, Ebert BL, Gillette MA, Paulovich A, Pomeroy S, Golub TR, Lander ES, et al. Gene set enrichment analysis: a knowledge-based approach for interpreting genome-wide expression profiles. *Proc Natl Acad Sci U S A*. 2005;102(43):15545–15550. doi:10.1073/pnas.0506580102.
21. Otasek D, Morris JH, Bouças J, Pico AR, Demchak B. Cytoscape Automation: empowering workflow-based network analysis. *Genome Biol*. 2019;20(1):185. doi:10.1186/s13059-019-1758-4.
22. Garrido F, Aptsiauri N, Doorduijn EM, Garcia Lora AM, van Hall T. The urgent need to recover MHC class I in cancers for effective immunotherapy. *Curr Opin Immunol*. 2016;39:44–51. doi:10.1016/j.coi.2015.12.007.
23. Harms JS, Splitter GA. Interferon-gamma inhibits transgene expression driven by SV40 or CMV promoters but augments expression driven by the mammalian MHC I promoter. *Hum Gene Ther*. 1995;6(10):1291–1297. doi:10.1089/hum.1995.6.10-1291.
24. Dhar GA, Saha S, Mitra P, Nag Chaudhuri R. DNA methylation and regulation of gene expression: guardian of our health. *Nucleus*. 2021;64(3):259–270. doi:10.1007/s13237-021-00367-y.
25. Qasim W, Brunetto M, Gehring AJ, Xue S-A, Schurich A, Khakpoor A, Zhan H, Ciccorossi P, Gilmour K, Cavallone D, et al. Immunotherapy of HCC metastases with autologous T cell receptor redirected T cells, targeting HBsAg in a liver transplant patient. *J Hepatol*. 2015;62(2):486–491. doi:10.1016/j.jhep.2014.10.001.
26. Tan AT, Bertolotti A. HBV-HCC treatment with mRNA electroporated HBV-TCR T cells. *null*. 2021;2(1):ltab026. doi:10.1093/immadv/ltab026.
27. Kim CY, Tilles JG. Purification and biophysical characterization of hepatitis B Antigen. *J Clin Invest*. 1973;52(5):1176–1186. doi:10.1172/JCI107284.
28. Jiang M, Broering R, Trippler M, Poggenpohl L, Fiedler M, Gerken G, Lu M, Schlaak JF. Toll-like receptor-mediated immune responses are attenuated in the presence of high levels of hepatitis B virus surface antigen. *J Viral Hepat*. 2014;21(12):860–872. doi:10.1111/jvh.12216.
29. Riedl P, Reiser M, Stifter K, Krieger J, Schirmbeck R. Differential presentation of endogenous and exogenous hepatitis B surface antigens influences priming of CD8(+) T cells in an epitope-specific manner. *Eur J Immunol*. 2014;44(7):1981–1991. doi:10.1002/eji.201343933.
30. Tout I, Loureiro D, Mansouri A, Soumelis V, Boyer N, Asselah T. Hepatitis B surface antigen seroclearance: immune mechanisms, clinical impact, importance for drug development. *J Hepatol*. 2020;73(2):409–422. doi:10.1016/j.jhep.2020.04.013.
31. Fumagalli V, Di Lucia P, Venzin V, Bono EB, Jordan R, Frey CR, Chisari FV, Guidotti LG, Iannacone M, Iannacone M. Serum HBsAg clearance has minimal impact on CD8+ T cell responses in mouse models of HBV infection. *J Exp Med*. 2020;217(11):e20200298. doi:10.1084/jem.20200298.
32. Lee W-S, Lee K-W, Heo J-S, Kim S-J, Coi S-H, Kim Y-I, Joh J-W. Comparison of combined hepatocellular and cholangiocarcinoma with hepatocellular carcinoma and intrahepatic cholangiocarcinoma. *Surg Today*. 2006;36(10):892–897. doi:10.1007/s00595-006-3276-8.
33. Taguchi J, Nakashima O, Tanaka M, Hisaka T, Takazawa T, Kojiro M. A clinicopathological study on combined hepatocellular and cholangiocarcinoma. *J Gastroen Hepatol*. 1996;11(8):758–764. doi:10.1111/j.1440-1746.1996.tb00327.x.
34. Liu S, Zhang H, Gu C, Yin J, He Y, Xie J, Cao G. Associations between hepatitis B virus mutations and the risk of hepatocellular carcinoma: a meta-analysis. *J Natl Cancer Inst*. 2009;101(15):1066–1082. doi:10.1093/jnci/djp180.
35. Chu CM, Liaw YF. HBsAg seroclearance in asymptomatic carriers of high endemic areas: appreciably high rates during a long-term follow-up. *Hepatology*. 2007;45(5):1187–1192. doi:10.1002/hep.21612.
36. Simonetti J, Bulkow L, McMahon BJ, Homan C, Snowball M, Negus S, Williams J, Livingston SE. Clearance of hepatitis B surface antigen and risk of hepatocellular carcinoma in a cohort chronically infected with hepatitis B virus. *Hepatology*. 2010;51(5):1531–1537. doi:10.1002/hep.21612.
37. Moini M, Fung S. HBsAg loss as a treatment endpoint for chronic HBV infection: hBV cure. *Viruses*. 2022;14(4):657. doi:10.3390/v14040657.